Characterization and Application of Nanomaterials (2021) Volume 4 Issue 1
doi:10.24294/can.v4i1.1323

ORIGINAL RESEARCH ARTICLE

Spin thermoelectric effects of new-style one-dimensional carbon-based nanomaterials

Yushen Liu[1*], Jinfu Feng[1], Xuefeng Wang[2]

[1] *School of Physics and Electronic Engineering, Changshu Institute of Technology, Changshu 215500, China. E-mail: ysliu@cslg.edu.cn*

[2] *College of Physics, Optoelectronics and Energy, Soochow University, Suzhou 215006, China*

ABSTRACT

Based on first-principles methods, the authors of this paper investigate spin thermoelectric effects of one-dimensional spin-based devices consisting of zigzag-edged graphene nanoribbons (ZGNRs), carbon chains and graphene nanoflake. It is found that the spin-down transmission function is suppressed to zero, while the spin-up transmission function is about 0.25. Therefore, an ideal half-metallic property is achieved. In addition, the phonon thermal conductance is obviously smaller than the electronic thermal conductance. Meantime, the spin Seebeck effects are obviously enhanced at the low-temperature regime (about 80 K), resulting in the fact that spin thermoelectric figure of merit can reach about 40. Moreover, the spin thermoelectric figure of merit is always larger than the corresponding charge thermoelectric figure of merit. Therefore, the study shows that they can be used to prepare the ideal thermospin devices.

Keywords: Graphene Nanoribbons; Carbon Chains; Graphene Nanoflake; Spin Seebeck Coefficients; Thermoelectric Figure of Merit

ARTICLE INFO

Received: 15 November 2020
Accepted: 8 January 2021
Available online: 14 January 2021

1. Introduction

Carbon is one of the elements widely distributed in nature. As a tetravalent non-metallic element, it can form covalent bonds with metals and non-metals and combine into a variety of carbon-based nanomaterials. Graphene, as a two-dimensional allotrope of carbon, has been widely studied because of its unique electrical properties. Reviewing its development history, it is found that it has attracted early attention in theory, but the extensive research on its properties began with Geim and Novoselov, who obtained nearly perfect monolayer and free state graphene by simple mechanical method for the first time[1]. From the atomic level, graphene is composed of sp_2 hybrid carbon atoms. It is also an aromatic compound with a large π electron conjugate system. The special energy band structure leads to a semiconductor with zero energy gap. Unlike traditional semiconductor materials, graphene follows Dirac equation rather than Schrodinger equation. The migration rate of carriers in the conjugate system is very high, even close to the speed of light, making graphene one of the materials with the lowest resistivity at present.

Although graphene has very unique electrical properties, it cannot be directly used in logic devices due to the energy band structure of zero energy gap. In order to open the energy gap, a common method is

to shear two-dimensional graphene into one-dimensional nano band structure and introduce quantum confined domain effect and boundary effect. When the width is less than 10 nm, graphene nanoribbons will open the energy gap. The preparation methods of graphene nanoribbons can be divided into two kinds: one is the top-down synthesis method. For example, carbon nanotubes can be cut by physical or chemical methods using carbon nanotubes as basic raw materials. The other is the bottom-up synthesis method, that is, the nanoribbon structure is synthesized from small molecular raw materials. According to the boundary structure characteristics of the ribbons, graphene nanoribbons can be divided into two types: armchair and zigzag. Armchair nanoribbons (AGNRS) show non-magnetic semiconductor behavior, and the band gap decreases with the gradual increase of width[2]. Zigzag nanoribbons (ZGNRs) have spin-polarized boundary states due to the presence of non-bonding electrons in boundary carbon atoms. Theoretical study shows that the ground state of zigzag nanoribbons (ZGNRs) is that the boundary spin has antiferromagnetic order, that is, the directions of different boundary spins are opposite, but on the same side, the boundary spins show ferromagnetic arrangement. With a suitable applied magnetic field, we can realize the ferromagnetic order of different boundary spins[3]. Regardless of whether different boundary carbon atoms show ferromagnetic order or antiferromagnetic order, the density of states at the Fermi plane is spin degenerate, which limits their application in spintronics. However, using a transverse electric field, we can make ZGNRs realize semi-metallic property[4]. Here, the semi-metallic property refers to the fact that the Fermi surface shows an insulating state for one spin band structure and a metallic state for the other. In addition, the magnetic property and transport property of ZGNRs are also affected by chemical element doping or defect[5–7]. Interestingly, some studies show that a single spin negative differential resistance is found in the boundary doped ZGNRs[5].

In addition to voltage driving electrons or holes in materials to move at a certain direction, temperature difference can also drive electrons. More electrons or holes are often accumulated at the high and low temperature ends, so the voltage caused by temperature difference will appear in this material. This phenomenon is called Seebeck effect. Recently, with the progress of spin detection technology, K. Uchida, *et al.* firstly observed spin voltage caused by temperature difference in metal magnets, which is called spin Seebeck effect[8]. This pioneering experiment inspired people to theoretically study spin-related thermoelectric effects in various systems[9–21]. Recently, we have obtained high spin polarizability and large single spin Seebeck effect at the Fermi plane by doping ferromagnetic ZGNRs with boundary non-magnetic elements[16]. At present, a stable carbon atom chain (CAC) can be synthesized from graphene by electron irradiation technology using high-resolution transmission electron microscope[22]. Shen, *et al.* found that the channel transport property of CACs does not depend on structural deformation, structural defects and hydrogen adsorption[23]. Carbon-based nanostructures exhibit perfect spin filtering effect and giant magnetoresistance under near zero bias. Recently, Dong, *et al.* have studied the transport property of zigzag graphene nanoribbons connected with CACs[24]. It is found that the electron transport near the Fermi level can be changed by adjusting the position and the number of atoms in CACs. Fano resonance effect is an interference effect existing between the local state and the extended state. It was first found in the inelastic scattering of electrons in helium. In 2002, Kobayashi, *et al.* found that the adjustable Fano effect was observed in the Aharonov-Bohm ring embedded in quantum dots[25]. Two quantum dots can be coupled into an artificial molecule, and then the electrons will be shared by the two quantum dots. When the electron energy is close to Fano linear system, the Seebeck effect is significantly strengthened[26].

In this paper, the spin thermoelectric property of one-dimensional spin quantum devices composed of graphene nanoribbons, carbon chains and graphene nanosheets was studied. The first principle calculation shows that the spin-down transfer function at the Fermi face is suppressed to almost zero, however, the spin-up transfer function is close to 0.25.

Therefore, we got distinct semimetal property. In addition, the phonon partial thermal conductivity in the low-temperature region is significantly smaller than the corresponding electron partial conductance. However, in the low temperature region (near 80 K), the spin Seebeck coefficient is significantly strengthened, resulting in the charge and spin thermoelectric quality factor close to 40. Moreover, in the whole temperature range ($0 < T \leq 400$ K), the spin thermoelectric quality factor is always greater than the corresponding charge thermoelectric quality factor, and becomes more obvious in the room temperature region. Therefore, this one-dimensional carbon-based nanoribbon can be designed as an ideal spin thermoelectric device.

2. Model establishment

In this paper, a one-dimensional nano double probe system as shown in **Figure 1(a)** was designed. The left electrode and the right electrode are composed of serrated graphene nanoribbons, and the boundary carbon atoms are saturated with hydrogen atoms. The central scattering region is connected by a graphene nano sheet to a zigzag graphene nanoribbon through two carbon atom chains. The width of the graphene nanoribbon is represented by the number of carbon atoms perpendicular to the transport direction. In this paper, the width is 6.

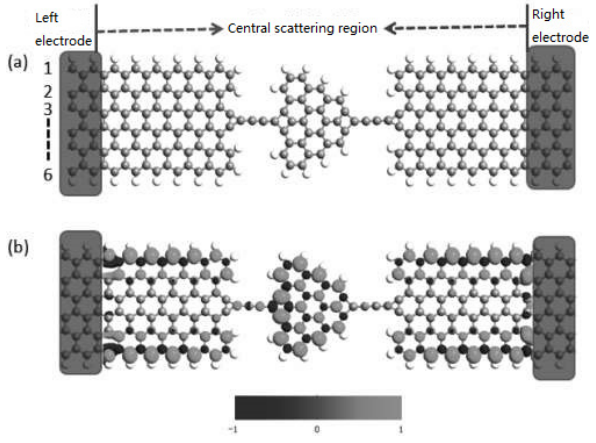

Figure 1. Thermal spin quantum double probe model and corresponding spin density.

All numerical calculations are completed based on the software package Atomistix Toolkit (ATK) of non-equilibrium Green's function and density functional theory[27–28]. The system optimization adopts Newton optimization method; the exchange correlation function adopts generalized gradient approximation (GGA), and the basis vector adopts DZP (Double-Zeta-Polarized). The size of the reduced Brillouin zone is set to (1, 1, 100). In order to avoid the interaction between images, the vacuum layer is taken as 15 Å and the truncation energy is taken as 150 Ry.

Using ATK software, the transmission coefficient of spin resolvable electrons with energy of E is:

$$\tau_\sigma(E) = T_r[\Gamma_{L\sigma}(E)G_\sigma^R(E)\Gamma_{R\sigma}(E)G_\sigma^A(E)] \quad (1)$$

Here, $\Gamma_{L/R\sigma}(E)$ is the linewidth function of the coupling between the central scattering region and the left/right electrode; σ is the spin index and E is the energy. $G_\sigma^{R(A)}(E)$ is the delayed and advanced Green's functions of the center scattering region. It can be determined by the equations

$G_\sigma^r = [EI - H + i(\Gamma_{L\sigma} + \Gamma_{R\sigma})/2]^{-1}$ and $G_\sigma^A = [Gr_\sigma^R]$. I is the identity matrix. H is the Hamiltonian of the central scattering region.

The spin polarizability at the Fermi plane is defined as:

$$\zeta = \frac{\tau_\uparrow(E)-\tau_\downarrow(E)}{\tau_\uparrow(E)+\tau_\downarrow(E)}\Big|_{E=E_f} \quad (2)$$

In order to study the spin thermoelectric effect, we give the expression of spin-dependent Seebeck coefficient in the linear region:

$$S_\sigma = -\frac{L_{1\sigma}(\mu,T)}{|e|TL_{0\sigma}(\mu,T)} \quad (3)$$

The thermal conductivity of the electronic part can be written as:

$$k_{el} = \sum_\sigma \left[K_{1\sigma}eS_\sigma + \frac{L_{2\sigma}}{T}\right]$$

Here, $L_n = \sum_\sigma L_{n\sigma}$, $L_{n\sigma} = -\frac{1}{h}\int dET_\sigma(E)(E-\mu)^n\frac{\partial f}{\partial E}$, $n = 0, 1, 2$. $f_{L(R)}$ is the Fermi Dirac distribution function. Spin Seebeck coefficient is expressed as $S_s = (S_\uparrow - S_\downarrow)/2$, and the corresponding charge Seebeck coefficient is $Sc = (S_\uparrow + S_\downarrow)/2$[14].

Charge (spin) thermoelectric quality factors are obtained from the following equation:

$$Z_{C(S)}T = \frac{S_{C(S)}^2 G_{e(S)}T}{\kappa_{el} + \kappa_{ph}} \quad (4)$$

$G_{e(S)}$ is the corresponding charge and spin con-

ductance, which can be obtained by the following equation:

$$G_{e(S)} = \frac{e^2}{h}(L_{0\uparrow} + (-)L_{0\downarrow}) \tag{5}$$

The phonon partial heat guide in formula (4) is available in the ATK2013 beta.

3. Results and discussion

Figure 1(b) shows that ZGNR still has boundary spin state in the buffer region, and the ferromagnetic order is maintained at the three boundaries of graphene nanosheets, that is, the spins of boundary carbon atoms are arranged in parallel. In **Figure 2(b)**, we draw the variation trend of spin resolvable transfer function with electron energy, and find a wide energy region near the Fermi plane (for example: –0.25 eV < E < 0.1 eV). The spin-up transfer function remains limited, while the spin-down transfer function is suppressed to zero. Therefore, this device shows obvious semi-metallic behavior, and the spin polarizability satisfies $\zeta = 1$. In order to reveal the physical reason behind it, we draw the spatial distribution of spin dependent local density of states at the Fermi surface in **Figures 2(c)** and **(d)**. Obviously, the spin-up local density of states is distributed in the whole central scattering region domain, including ZGNR, graphene nanosheets and carbon chains. However, the spin-down local density of states is only distributed in the ZGNR in the middle scattering region, and does not appear on carbon chains and graphene nanosheets. This result further confirmed the semi-metallic property at the Fermi plane. We also found that the spin-up Fano type tunneling spectrum appears in the –0.2 eV region below the Fermi plane, but the spin-down Fano type tunneling spectrum appears at 0.1 eV on the Fermi plane. The corresponding trend of density of state with energy shows that these Fano type tunneling spectra come from the local state in the energy region (**Figure 2(a)**). Fano resonance is formed when these local states and surrounding electronic states undergo quantum interference effect.

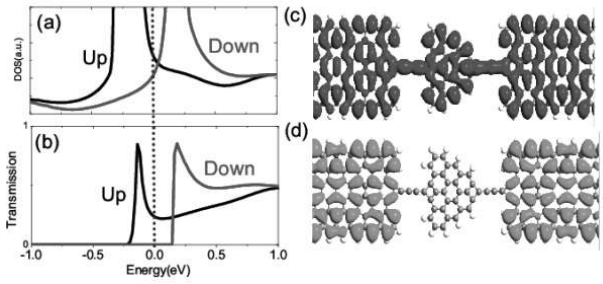

Figure 2. The spin-dependent transport property. **(a)** and **(b)** represent the variation trend of state density and transport function with the electron energy respectively, and the dashed line represents the position of the Fermi plane, letting the energy of the Fermi surface be zero. **(c)** and **(d)** indicate the local spin-up and spin-down density of states at the Fermi surface, respectively.

Fano resonance causes the transfer function to change dramatically with the electron energy, which is bound to strengthen the thermoelectric effect. Compared with other energy points, the thermoelectric performance at the Fermi surface will attract more attention of researchers. In **Figure 3(a)**, we give the change of spin-dependent Seebeck coefficient with temperature at the Fermi surface. It is found that the spin-up Seebeck coefficient is positive while the spin-down Seebeck coefficient is negative. This result can be well explained by the following equation. At low temperature, equation (3) can be simplified as:

$$S_\sigma(E_F) \simeq -\frac{\pi^2 k_B^2 T}{3e}[\ln \tau_\sigma(E)]'|_{E=E_F} \tag{6}$$

This equation shows that S_σ at the Fermi surface is directly proportional to the negative value of the slope of the transmission probability τ_σ and inversely proportional to its size. At the same time, we also note that it is directly proportional to the temperature T. This equation can well explain the behavior of S_σ in the low temperature region ($0 < T \leq 50$ K). However, when the temperature further increases, we find that the spin-down Seebeck coefficient is significantly strengthened, and equation (6) becomes no longer applicable. It is mainly because more nonlinearity participates in the contribution to the spin Seebeck coefficient at high temperature[29]. In order to calculate the charge and spin thermoelectric quality factors, in **Figure 3(b)**, we give the contribution of the

electron and phonon part to the thermal conductivity. The thermal conductivity contributed by the phonon part κ_{ph} and the thermal conductivity contributed by the electron part κ_{el} increase monotonically with the increase of temperature.

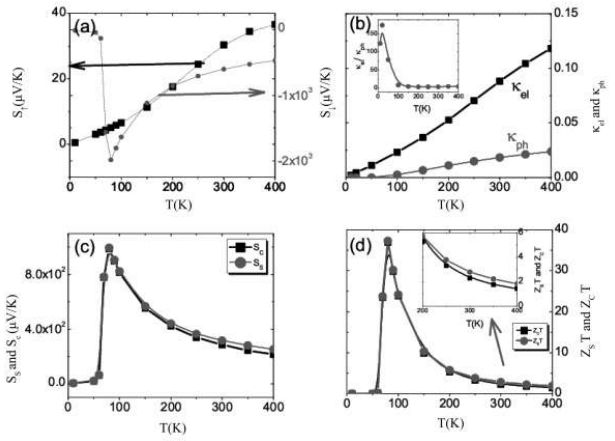

Figure 3. Spin-dependent thermoelectric property. **(a)** Spin-dependent Seebeck coefficients; **(b)** Electron and phonon partial thermal conductivity; **(c)** Charge and spin Seebeck coefficients; **(d)** Trend of spin and charge thermoelectric quality factors with temperature.

Moreover, it is important that the thermal conductivity of the phonon part is significantly lower than that of the electronic part, especially in the low temperature region (T < 100 K), and the thermal conductivity of the phonon part is one percent of the electronic part (See the embedded diagram in **Figure 3(b)**). Interestingly, the spin-down Seebeck coefficient is significantly strengthened near the temperature of 80 K, and the maximum value even reaches 2000 μV/K. The charge Seebeck coefficient S_c and spin Seebeck coefficient S_s are also significantly strengthened near the temperature of 80 K. In the high temperature region (near room temperature), we find that the value S_s is significantly larger than S_c, which indicates that the spin thermoelectric effect is significantly stronger than the corresponding charge thermoelectric effect. In **Figure 3(d)**, we show the variation trend of spin thermoelectric quality factor Z_ST and charge thermoelectric quality factor Z_CT with temperature T. The results show that their maximum value is close to 40, and the sizes of Z_ST and Z_CT are the same in the whole temperature region. Generally speaking, if the thermoelectric quality factor is greater than 3, it is considered that the material has high thermoelectric efficiency. It can be used as an ideal thermoelectric material. More interestingly, in the high temperature region (room temperature region), Z_ST is significantly larger than Z_CT, and Z_ST is close to 3. This shows that this double probe model with carbon atoms can be used as an ideal thermoelectric device at room temperature.

4. Conclusion

We designed a one-dimensional spin quantum device composed of graphene nanoribbons, carbon chains and graphene nanosheets. It is found that the spin-down transfer function at the Fermi surface is almost suppressed to zero, while the spin-up transfer function is close to 0.25, so it has obvious semi-metallic property. In addition, we also found that in this device, the thermal conductivity of the phonon part is significantly smaller than the corresponding electronic partial conductance. In the low temperature region, the phonon partial thermal conductance is only one percent of the electronic partial thermal conductance. However, in the low temperature region (near 80 K), the spin Seebeck coefficient is significantly strengthened, resulting in the charge or spin quality factor close to 40. Moreover, in the whole temperature range (0< $T \leq$ 400 K), the spin thermoelectric quality factor is always greater than the corresponding charge thermoelectric quality factor, and this effect becomes more obvious at room temperature. Therefore, this one-dimensional carbon-based nanoribbon can be used to design ideal spin thermoelectric devices at room temperature.

Conflict of interest

The authors declare that they have no conflict of interest.

Acknowledgements

National Natural Science Foundation of China "Research on theory and application of molecular thermoelectric devices" (11247028).

References

1. Novoselov KS, Geim AK, Morozov SV. Electric field effect in atomically thin carbon films. Science 2004; 306: 666–669.
2. Son Y, Cohen ML, Louie SG. Energy gaps in graphene nanoribbons. Physical Review Letters 2007; 98(8).
3. Xu C, Luo G, Liu Q, *et al.* Giant magnetoresistance in silicene nanoribbons. Nanoscale 2012; 4: 3111–3117.
4. Son Y, Cohen ML, Louie SG. Half-metallic graphene nanoribbons. Nature 2006; 444: 347.
5. Wu T, Wang X, Zhai M, *et al.* Negativedifferential spin conductance in doped zigzag graphenenanoribbons. Applied Physical Letters 2012; 100(5): 2112.
6. Maunárriz J, Gaul C, Malyshev AV, *et al.* Strong spin-dependent negative differential resistance in composite graphene superlattices. Physical Review B Condensed Matter 2012; 88(15): 5423.
7. Jiang C, Wang X, Zhai M. Spin negative differential resistance in edge doped zigzag graphene nanoribbons. Carbon an International Journal Sponsored by the American Carbon Society 2014; 68: 406.
8. Uchida K, Takahashi S, Harii K, *et al.* Observation of the spin Seebeck effect. Nature 2008; 455: 778.
9. Dubi Y, Di Ventra M. Thermo-spin effects in a quantum dot connected to ferromagnetic leads. Physical Review B Condensed Matter 2009; 79(8): 1302(R).
10. Jaworski CM, Yang J, Mack S, *et al.* Observation of spin-Seebeck effect in a ferromagnetic semiconductor. Nature Mater 2010; 9: 898.
11. Uchida K, Adachi H, *et al.* Long-range spin Seebeck effect and acoustic spin pumping. Nature Mater 2011; 10: 737.
12. Adachi H, Ohe J, Takahashi S, *et al.* Linear-response theory of spin Seebeck effect in ferromagnetic insulators. Physical Review B 2011; 83(9): 4410.
13. Dubi Y, Di Ventra M. Colloquium: Heat flow and thermoelectricity in atomic and molecular junctions. Review of Modern Physics 2011; 83: 131.
14. Liu Y, Chi F, Yang X, *et al.* Pure spin thermoelectric generator based on a rashba quantum dot molecule. Journal of Applied Physics 2011; 109(5): 3712.
15. Liu Y, Yang X, Chi F, *et al.* A proposal for time-dependent pure-spin-current generators. Applied Physics Letters 2012; 101(21): 3109.
16. Liu Y, Wang X, Chi F. Non-magnetic doping induced a high spin-filter efficiency and large spin Seebeck effect in zigzag graphene nanoribbons. Journal of Materials Chemistry C 2013; 2013(1): 3756–3776.
17. Yang X, Liu Y, Zhang X, *et al.* Perfect spin filtering and large spin thermoelectric effects in organic transition-metal molecular junctions. Physical Chemistry Chemical Physics Cambridge Royal Society of Chemistry 2014; 16: 11349–11357.
18. Liu Y, Zhang X, Wang X, *et al.* Spin-resolved Fano resonances induced large spin Seebeck effects in grapheme carbon-chain junctions. Applied Physics Letters 2014; 104(24): 2412.
19. Yang X, Liu Y, Wang X, *et al.* Large spin Seebeck effects in zigzag-edge silicene nanoribbons. Aip Advances 2014; 4(8): 7116.
20. Yang X, Zhang X, Hong X, *et al.* Temperature-controlled giant thermal magnetoresistance behaviors in doped zigzagedged silicene nanoribbons. Rsc Advances 2014; 4: 48539–48546.
21. Yang X, Zhou W, Hong X, *et al.* Half-metallic properties, single-spin negative differential resistance, and large singlespin Seebeck effects induced by chemical doping in zigzag-edged graphene nanoribbons. The Journal of Chemical Physics 2015; 142(2): 4706.
22. Jin C, Lan H, Peng L, *et al.* Deriving carbon atomic chains from graphene. Physical Review Letters 2009; 102(20): 5501.
23. Shen L, Zeng M, Yang S, *et al.* Electron transport properties of atomic carbon nanowires between graphene electrodes. Journal of the American Chemical Society 2010; 132: 11481–11486.
24. Dong Y, Wang X, Zhai M, *et al.* Half-metallicity in aluminum-doped zigzag silicene nanoribbons. The Journal of Physical Chemistry C 2013; 117(37): 18845–18850.
25. Kobayashi K, Aikawa H, Katsumoto S, *et al.* Tuning of the Fano effect through a quantum dot in an Aharonov-bohm Interferometer. Physics Review Letters 2002; 88: 256806.
26. Liu Y, Yang X. Enhancement of thermoelectric efficiency in a double-quantum-dot molecular junction.

Journal of Applied Physics 2010; 108(2): 3710.
27. Taylor T, Guo H, Wang J. Ab initio modeling of quantum transport properties of molecular electronic devices. Physical Review B 2001; 63(24): 5407.
28. Brandbyge M, Mozos JL, Ordejon P, *et al.* Density-functional method for non-equilibrium electron transport. Physical Review B, Condensed Matter 2002; 65(16): 5401.
29. Yang X, Liu Y. Pure spin current in a double quantum dot device generated by thermal. Journal of Applied Physics 2013; 113(16): 4310.